ELSEVIER

Journal of Contaminant Hydrology 41 (2000) 23–47

JOURNAL OF Contaminant Hydrology

www.elsevier.com/locate/jconhyd

Modelling of sulfide oxidation with reactive transport at a mine drainage site

J.G. Bain *, D.W. Blowes [1], W.D. Robertson, E.O. Frind

Department of Earth Sciences, University of Waterloo, Waterloo, Ontario, Canada, N2L 3G1

Received 30 June 1997; received in revised form 15 June 1999; accepted 19 July 1999

Abstract

A plume of groundwater affected by sulfide oxidation extends 160 m downgradient from the Nickel Rim Mine tailings impoundment and discharges to a small lake. The plume water has near neutral pH, but contains high concentrations of Fe and SO_4. Field observations indicate that the release of SO_4, H^+, Fe^{2+} and other metals and their distribution in the aquifer is controlled by the rate of sulfide oxidation in the vadose zone of the tailings and by subsequent dissolution and precipitation of carbonate and oxyhydroxide mineral phases in the tailings and aquifer. Using field-determined aqueous and solid geochemistry, a conceptual geochemical model for the site was developed. This model accounts for trends in pH and in the concentrations of Fe and SO_4. The numerical model MINTOX was used in conjunction with this conceptual model to simulate sulfide oxidation and two-dimensional reactive transport of dissolved sulfide oxidation products. Simulated sulfide oxidation and transport are compared to trends observed in the field after 35 years of oxidation. Similarity between observed and simulated concentrations demonstrates that, when used with a well-developed conceptual geochemical model, MINTOX is capable of simulating sulfide oxidation and plume evolution at mine drainage sites.

Keywords: Mine drainage; Sulfide oxidation; Reactive solute transport; Geochemical modelling

1. Introduction

The diffusion of oxygen into the pore space of the vadose zone of the decommissioned tailings impoundment at the Nickel Rim Mine site near Sudbury, Ontario has resulted in the oxidation of sulfide minerals, predominantly pyrrhotite ($Fe_{1-x}S$). Sulfide

* Corresponding author. Tel.: +1-519-888-4878; fax: +1-519-746-3882; E-mail: jbain@sciborg.uwaterloo.ca

[1] E-mail: blowes@sciborg.uwaterloo.ca.

0169-7722/00/$ - see front matter
PII: S0169-7722(99)00069-8

oxidation has released high concentrations of sulfate (SO_4) and ferrous iron (Fe(II)), which now form a plume in the impoundment and the underlying sand aquifer (Johnson et al., 2000). The aquifer discharges along seepage faces adjacent to the impoundment, and to Moose Lake, which is 160 m downgradient from the impoundment. At the tailings surface, the oxidation of Fe(II) and subsequent precipitation of iron oxyhydroxide phases releases H^+. Because high concentrations of Fe(II) can remain dissolved in water at neutral or low pH, the transport of Fe(II) along the groundwater flow path represents a mechanism of transporting potential acidity over long distances. At Nickel Rim and at many other mining locations, the discharge of water containing high concentrations of Fe(II) to the surficial environment has caused degradation of water quality (Cherry et al., 1982; Filipek et al., 1987; Bain, 1996).

Johnson et al. (2000) developed a conceptual model that describes the geochemical reactions controlling the geochemistry of the advancing plume water within the tailings impoundment. Bain (1996) extended the conceptual model into the unconfined aquifer which underlies the impoundment. In the conceptual model, the pH of advancing plume water is gradually neutralized through a sequence of carbonate and hydroxide mineral dissolution reactions. The concentrations of Fe, Al, SO_4 and other dissolved species are controlled by the formation of secondary solid phases, in response to changing pH and redox conditions.

The set of acid-base, redox and dissolution-precipitation reactions that occur simultaneously as plume water advances through the tailings and aquifer is complex, making it difficult to predict how the geochemistry of the water will evolve. Plume evolution is further complicated by changes in the rate of sulfide oxidation and the release of products (Fe, SO_4, H^+) as the tailings age, and complexity in the flow system.

MINTOX (Wunderly et al., 1996) is a numerical model that was designed to simulate kinetically controlled oxidation of sulfide minerals and subsequent reactive transport of sulfide oxidation products and other dissolved constituents through tailings and aquifer sediments. MINTOX combines the numerical models PYROX (Wunderly et al., 1996) and MINTRAN (Walter et al., 1994a,b). MINTRAN combines a two-dimensional (2-D), finite element, solute transport computer model (PLUME2D; Frind et al., 1990), with the geochemical speciation/mass transfer model MINTEQA2 (Allison et al., 1990). MINTRAN assumes local equilibrium (Walter et al., 1994a,b), wherein the reactions simulated are assumed to proceed sufficiently rapidly that local chemical equilibrium exists at all points (Rubin, 1983). In practical terms, equilibrium must be attained within the time step of the transport solution. MINTRAN requires the specification of a realistic transport scenario, specification of the geochemical processes in action and quantification of the aqueous, gaseous and solid-phase component masses.

The loading of sulfide oxidation products to the tailings pore-water is dependent on the rate of oxidation of sulfide minerals (Blowes and Jambor, 1990). Field studies have demonstrated that the rate of oxidation is controlled by the rate of oxygen diffusion into the tailings (Jaynes et al., 1984; Blowes and Jambor, 1990; Blowes et al., 1991). Several numerical models have been developed to describe sulfide oxidation in mine wastes and heap leach piles (Jaynes et al., 1984; Davis and Ritchie, 1986). PYROX is a one-dimensional (1-D), finite element numerical model designed to simulate the oxidation of sulfide minerals. PYROX is based on the conceptual model Davis and Ritchie (1986) in

which the overall rate of sulfide oxidation is controlled by the rate of diffusion of O_2 gas from the tailings impoundment surface to the depth of oxidation and by the rate of oxidant transport through a secondary iron-oxyhydroxide rim which surrounds the primary sulfide mineral. PYROX incorporates spatially variable diffusion coefficient values, sulfide contents, porosities and moisture contents. It is well suited to describe sulfide oxidation in partly saturated mine tailings. The gradual decline in $O_{2(g)}$ concentration vs. depth and the identification of rims of oxidized material on sulfide grains from the oxidation zone (Jambor and Owens, 1993) suggests that this model of sulfide oxidation is reasonable at Nickel Rim.

MINTOX has previously been used to simulate sulfide oxidation and the transport of oxidation products at the Nordic Uranium mine tailings impoundment, Elliot Lake, Ontario (Wunderly et al., 1996). Possible applications of the model might include the evaluation the benefits of proposed remedial programs at similar sulfide-tailings disposal sites, for example, the application of surface covers or the addition of pH buffering minerals during or after discharge.

In this paper, we use MINTOX to simulate development of the pH, Fe, SO_4 and Al plumes at Nickel Rim. Field observations were made at Nickel Rim approximately 35 years after the onset of sulfide oxidation. These field data are a basis of comparison to the model results. To apply MINTOX to Nickel Rim, the sequence of controlling reactions was discerned from field data and mineralogical observations. Although the reaction sequence is not unique, it does include mechanisms that control the evolution of pH trends and plumes of Al, Fe and SO_4 at the site, and it is consistent with measurements of pore-water chemistry (Bain, 1996; Johnson et al., 2000), and with the results of a detailed mineralogical study of the tailings impoundment (Jambor and Owens, 1993; Johnson et al., 2000).

The objectives of the simulations are (1) to assess the ability of MINTOX to accurately simulate the reaction sequence of the Nickel Rim conceptual model, and (2) to assess whether the conceptual model of controlling geochemical reactions, as simulated by MINTOX, describes field conditions (pH, Fe, Al and SO_4 plumes) observed at the Nickel Rim site.

The point of this modelling is not to prove that the conceptual model of Bain (1996) and Johnson et al. (2000) is correct or that the observed plume can be simulated exactly. The modelling exercise was conducted to demonstrate that using a well-developed conceptual model, MINTOX is capable of simulating sulfide oxidation and plume evolution at a mine drainage site. If, using the conceptual model for the site, MINTOX is able to simulate the observed geochemical plumes, it is probable that the conceptual model of Bain (1996) and Johnson et al. (2000) is correct, although not unique. Lack of agreement between simulated and observed plumes may reflect deficiencies in the conceptual model (missed or incorrect reactions), inaccuracies in the flow model used for the site, or an inability of MINTOX to correctly simulate the described reactions.

2. Physical and hydrogeologic setting

The Nickel Rim Mine is 35 km northeast of Sudbury, Ontario (Fig. 1). During mining operations between 1953 and 1958, pyrrhotite-rich tailings were deposited in nearby

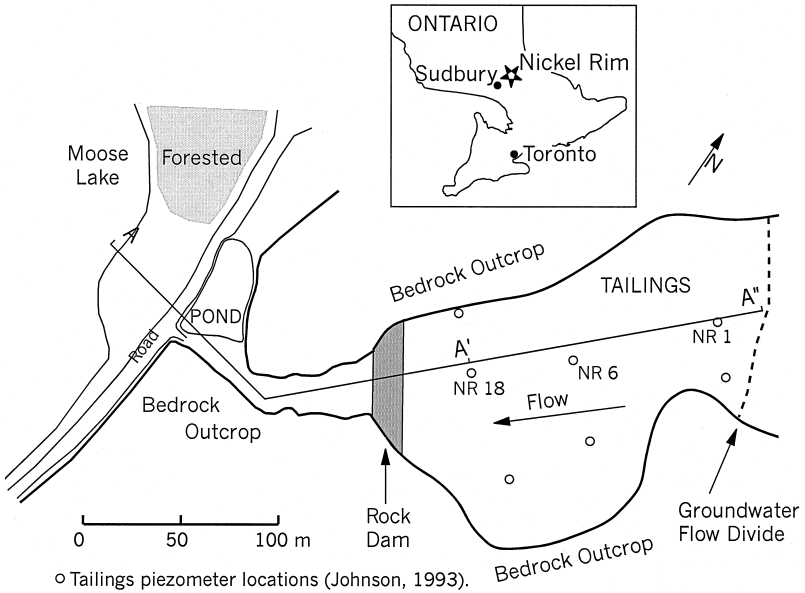

Fig. 1. Nickel Rim tailings and aquifer location. Longitudinal section and flow modelling done along section A–A″.

bedrock valleys, forming elevated impoundments (Thomson, 1961). The unoxidized tailings contain 0.5 to 5 wt.% S, and a low carbonate content of between 0.1 and 3 wt.%, as $CaCO_3$ (Johnson, 1993). A 3 to 8-m-thick aquifer underlying the impoundment is composed of silty, fine sand with local gravel-sized and boulder-sized material (Fig. 2). This aquifer is confined laterally to widths of 20 to 75 m by bedrock. The aquifer sediments are predominantly quartz and feldspar, with up to 0.6 wt.% carbonate, reported as $CaMg(CO_3)_2$. Carbonate minerals in the tailings and aquifer have a mixed Ca–Mg–Fe composition.

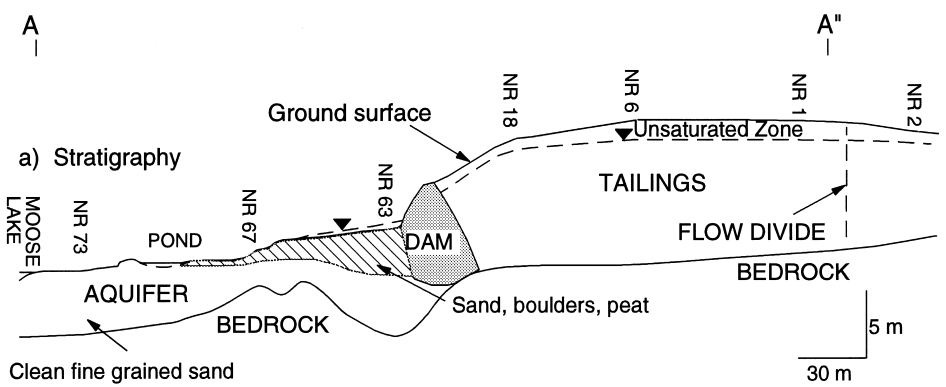

Fig. 2. Longitudinal view of the tailings and aquifer showing general stratigraphy and water table position.

A groundwater flow divide separates the impoundment into two flow systems, one flowing westward through a tailings dam to Moose Lake, and one flowing eastward to Lake Wanapitei (Fig. 1). This paper focuses on the flow system to Moose Lake. 2-D flow modelling conducted by Johnson (1993) and Bain (1996) suggests that in this flow system, ~50% of the precipitation recharge water is discharged to surface near the toe of the tailings dam, and ~50% flows through the aquifer to Moose Lake.

3. Summary of the conceptual model

Reactions that are included in the conceptual model for Nickel Rim were selected based upon field observations, mineralogical data and geochemical modelling results. Geochemical modelling with MINTEQA2 was used to infer the mineral phases potentially limiting the aqueous concentration of dissolved constituents. The modelling results, in conjunction with the results of an independent mineralogical study conducted by Jambor and Owens (1993), indicated that important minerals include calcite ($CaCO_3$), dolomite ($CaMg(CO_3)_2$), siderite ($FeCO_3$), gibbsite ($Al(OH)_3$, ferrihydrite ($Fe(OH)_3$), jarosite ($KFe_3(SO_4)_2(OH)_6$) and gypsum ($CaSO_4 \cdot 2H_2O$). Dissolution and precipitation of these minerals, in addition to the oxidation of pyrrhotite by O_2 and by ferric iron, were determined to be the primary mechanisms controlling the pH and Eh and the concentrations of Fe, Al and SO_4 in the tailings and aquifer (Bain, 1996; Johnson et al., 2000).

3.1. Sulfide oxidation

The diffusion of atmospheric oxygen into the vadose zone of the impoundment leads to the bacterially mediated oxidation of pyrrhotite, releasing Fe, SO_4 and H^+ to the pore-water (Fig. 3; Johnson et al., 2000):

$$Fe_{1-x}S + (2 - x/2)O_2 + xH_2O \Rightarrow (1 - x)Fe^{2+} + SO_4^{2-} + 2xH^+. \quad (1)$$

Near the surface of the impoundment, in the presence of oxygen, the Fe^{2+} produced from Eq. (1) may be oxidized to Fe^{3+}:

$$Fe^{2+} + 1/4O_2 + H^+ \Rightarrow Fe^{3+} + 1/2H_2O. \quad (2)$$

At Nickel Rim, Fe^{3+} generated by sulfide oxidation precipitates as goethite (α-FeOOH), poorly crystalline $Fe(OH)_3$, or jarosite ($KFe_3(SO_4)_2(OH)_6$) according to the reactions (Johnson et al., 2000):

$$Fe^{3+} + 2H_2O \Leftrightarrow FeOOH + 3H^+, \quad (3)$$

$$K^+ + 3Fe^{3+} + 2SO_4^{2-} + 6H_2O \Leftrightarrow KFe_3(SO_4)_2(OH)_6 + 6H^+. \quad (4)$$

The highest concentrations of sulfide oxidation products were probably released within a few years after tailings disposal ceased, as oxygen diffused into the fresh tailings. Mineralogical examination of the tailings indicates that alteration rims of oxidized material surround and replace the primary sulfide grains from the vadose zone

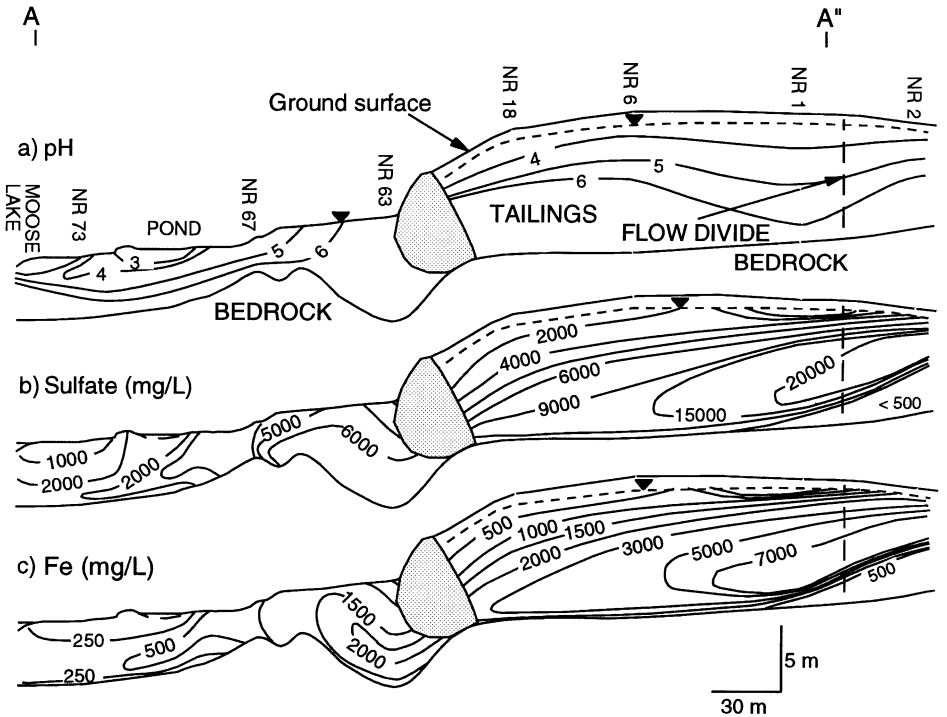

Fig. 3. Longitudinal view of the tailings and aquifer showing (a) pH values (b) dissolved Fe and (c) dissolved sulfate.

of the tailings (Jambor and Owens, 1993). The rate of release of sulfide oxidation products decreases gradually with time as the thickness of the oxidized coating around the sulfide particles increases, and as the transport distance from the surface of the impoundment to the depth of active oxidation increases (Davis and Ritchie, 1986).

Below the depth of oxygen diffusion in the tailings, anaerobic conditions favour the oxidation of pyrrhotite by Fe^{3+} through reactions of the form:

$$Fe_{1-x}S + 8Fe^{3+} + 4H_2O \Rightarrow (9-x)Fe^{2+} + SO_4^{2-} + 8H^+. \quad (5)$$

Below the oxidation zone, reactions 3, 4 and 5 limit Fe(III) concentrations to low values (Johnson et al., 2000). Reaction 5, which may be bacterially mediated, occurs quickly in comparison to the oxidation of pyrite by oxygen, and can produce high concentrations of Fe^{2+}, SO_4 and acidity (Stumm and Morgan, 1981).

3.2. Acid neutralization / metal attenuation

Field observations at Nickel Rim indicate that the transport of low-pH conditions along the groundwater flow path is limited by the dissolution of primary minerals

initially contained in the tailings and aquifer, and by the precipitation and dissolution of secondary minerals along the groundwater flow path. As acidic water that was affected by sulfide oxidation is displaced downward through the vadose zone and into deeper parts of the tailings and aquifer, the pH is gradually neutralized. In order of increasing depth below surface, a series of pH-buffered zones are observed at pH values of approximately 6.7, 5.6, 4.1 and 3.0 (Figs. 3 and 4; Johnson et al., 2000). These plateaus are attributed to the successive depletion of calcite, siderite, gibbsite and iron oxyhydroxides (ferrihydrite; Fig. 4). Buffering at pH values of between 2 and 3 immediately below the tailings surface is attributed to the dissolution of a combination of mineral phases, such as ferrihydrite, goethite, jarosite and aluminosilicates (Johnson et al., 2000). This reaction sequence is similar to that found at other mine drainage sites (Dubrovsky et al., 1984; Morin et al., 1988; Blowes et al., 1992).

The transport of dissolved metals is affected as these minerals precipitate and dissolve with the changing pH conditions. Geochemical modelling suggests that siderite should precipitate as dolomite/calcite dissolves. The front of dolomite/calcite dissolution and siderite precipitation is currently located near the base of the impoundment and near the tailings dam (Fig. 5; Johnson et al., 2000). Mineralogical study could not confirm the presence of siderite in the tailings or aquifer, nor could it discount the possibility of its presence (Johnson et al., 2000). This may be a result of a low total carbonate concentration (0–5 wt.%) in the tailings and aquifer, or may be a result of the difficulty in detecting and identifying poorly crystalline iron carbonate phases. The low concentration of solid phase carbonate in the tailings and aquifer limits the extent of siderite precipitation. As the low pH plume advances, sequential precipitation and

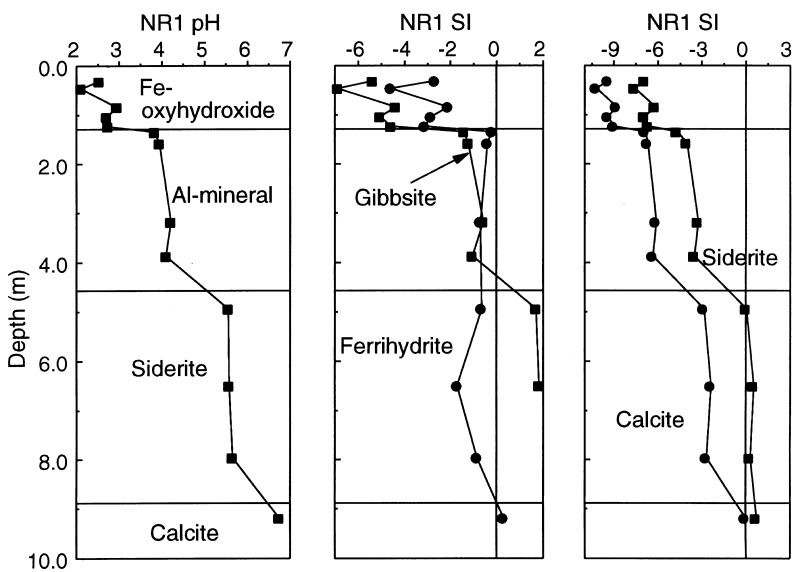

Fig. 4. Saturation indices for ferrihydrite, gibbsite, siderite and calcite, with corresponding pH values and indicated pH-buffering zones at NR 1, in the tailings (after Johnson, 1993).

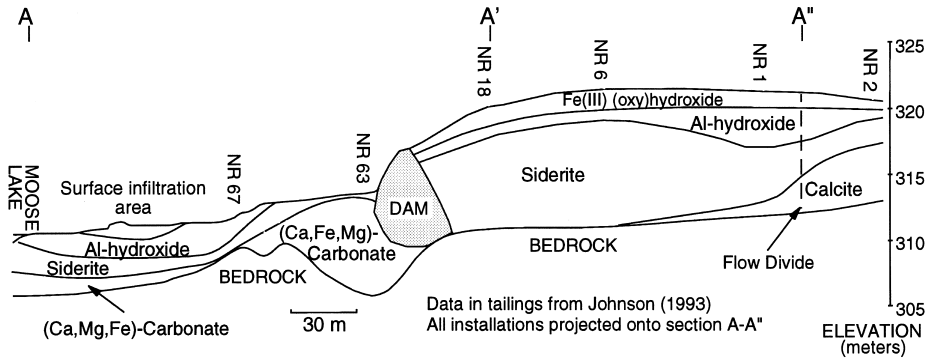

Fig. 5. Current location of pH buffering zones within the tailings and aquifer.

dissolution of siderite may limit the of movement of the Fe(II). Although the Fe(II) concentration is limited, it remains high and concentrations of 1500 to 2200 mg/l are subsequently displaced into the aquifer.

Aluminum is released to pore-water in the oxidation zone due to dissolution of aluminosilicate minerals (principally biotite) under low pH conditions (Johnson et al., 2000). Geochemical modelling of the field data suggests that Al concentrations in the tailings and aquifer are limited by the precipitation of secondary gibbsite or amorphous $Al(OH)_3$. These precipitation reactions occur within 3 to 5 m below the oxidation zone (Fig. 5). Geochemical calculations indicate that this infiltrating water is undersaturated with respect to siderite and supersaturated with respect to gibbsite. Although a secondary Al hydroxide phase was not detected in the tailings or aquifer, changes in the aqueous concentrations of Al are consistent with the formation of $Al(OH)_3$ or an analogous phase. In the zone where *am*-$Al(OH)_3$ is inferred to occur, the pH is maintained near 4 (Fig. 4).

The transport of dissolved SO_4 is sensitive to the precipitation and dissolution of the carbonate minerals and gypsum. Gypsum has been isolated from the tailings, suggesting that SO_4 concentrations in the tailings are limited by gypsum precipitation (Johnson et al., 2000). Although the groundwater is at equilibrium with respect to gypsum, the high solubility of this mineral results in high concentrations of dissolved SO_4 in the tailings and aquifer (2000 to 7000 mg/l). Dispersion and historic variations in the rate of oxidation also result in decreasing SO_4 concentrations downgradient from the oxidation zone.

4. Application of the MINTOX model

4.1. Incorporation of the conceptual model

The application of MINTOX requires the specification of the initial concentration of a large number of solid-phase and dissolved components. The initial values of these

input parameters are poorly quantified at the Nickel Rim tailings impoundment. It is not possible, for example, to determine the original mineralogy of the tailings, the historical development of the vadose zone, or the initial composition of the tailings water. Because these parameters cannot be independently determined, a series of parameter values within the range of those observed at the field site was specified. Where specific values could not be assigned, parameters were selected using sensitivity analyses (Bain, 1996). The MINTOX simulations account for the reactive transport of the major dissolved constituents in the Nickel Rim groundwater; however, in this paper, we focus on the model results for pH and the contaminants Fe, Al and SO_4.

With the exception of aluminosilicate mineral dissolution reactions, we have incorporated the reactions described in the conceptual model for Nickel Rim (Sections 3.1 and 3.2) into MINTOX to control the behaviour of pH, Fe, Al and SO_4. Aluminosilicate minerals dominate the composition of the Nickel Rim tailings, and their dissolution is typically an important pH-buffering mechanism in mine tailings (Blowes and Ptacek, 1994; Ptacek and Blowes, 1994). These minerals, however, are slow to dissolve, and equilibrium with respect to passing pore-water generally is not attained. Minerals, such as aluminosilicates, which may be kinetically inhibited from dissolving, are not correctly modelled with an equilibrium approach, and are not included in the MINTOX simulations.

Models that consider both kinetic and equilibrium reactions have recently been developed. The models HYDROGEOCHEM2 (Yeh and Salvage, 1997) and MIN3P (Mayer, 1999) incorporate both equilibrium and kinetically controlled reactions with multicomponent 2-D groundwater transport. Broshears et al. (1996) demonstrated in a surface water reactive transport model the importance of employing kinetic controls on the dissolution of selected minerals.

Although pyrrhotite oxidation can be simulated by PYROX, difficulties were encountered in equilibrating the resulting water in MINTOX. The same difficulties were not encountered using the ferrous sulfide mineral pyrite (FeS_2), however. As a result, pyrrhotite oxidation was simulated in MINTOX by using pyrite as a surrogate for pyrrhotite. Pyrite oxidation occurs according to the reactions:

$$FeS_2 + H_2O + 7/2O_2 \Rightarrow Fe^{2+} + 2SO_4^{2-} + 2H^+, \quad (6)$$

$$FeS_2 + 1/2H_2O + 15/4O_2 \Rightarrow Fe^{3+} + 2SO_4^{2-} + H^+. \quad (7)$$

Although pyrrhotite and pyrite oxidation produce slightly different quantities of Fe, SO_4 and H^+, it is anticipated that these stoichiometric variations are within the range of uncertainty of the mineralogical composition of the tailings (0.5–5 wt.% S content as pyrrhotite; Johnson, 1993).

The anaerobic oxidation of pyrrhotite and other sulfide minerals by Fe^{3+} is important at Nickel Rim (Johnson et al., 2000). Below the depth of oxygen diffusion in the tailings, anaerobic oxidation of pyrite by Fe^{3+} occurs through reactions of the form:

$$FeS_2 + 14Fe^{3+} + 8H_2O \Rightarrow 15Fe^{2+} + 2SO_4^{2-} + 16H^+. \quad (8)$$

Although this reaction is kinetically limited, it occurs rapidly when bacterially mediated (Stumm and Morgan, 1981; Nicholson, 1994). For the purpose of these simulations, it is

assumed that the anaerobic oxidation of pyrrhotite is not rate limited, and occurs rapidly compared to groundwater transport rates. As with the anaerobic oxidation of pyrrhotite (reaction 5), reactions 3, 4 and 8 limit Fe(III) concentrations below the oxidation zone.

4.2. Background-solid geochemistry

Simulations were based on the composition of the solids and pore-water observed in the tailings at present, in deep areas in the impoundment, and in distal parts of the aquifer (Table 1). Except for the sulfide content of the tailings, the composition of the tailings and of the aquifer are assumed to be similar. With the exception of the oxidation zone, the background composition is assumed to be uniform through the tailings, the dam and the aquifer. All solids in the tailings and aquifer are assumed to be pure, and uniformly distributed.

Pyrite is present only in the upper 0.7 m of the impoundment, where it can be oxidized by oxygen within the zone of oxygen infiltration. Pyrrhotite in the model is present only below the depth of oxygen infiltration, where it is oxidized by Fe^{3+} (Table 1).

For the simulation, the initial carbonate mass in the tailings and aquifer is assumed to be comprised of a mixture of dolomite plus siderite, totalling 0.01 wt.% as $CaCO_3$ (Table 1).

Aluminosilicate dissolution in the low pH zone is a primary source of Al, Ca, K, Mg, Na and Si in the tailings water (Johnson et al., 2000). The exclusion of aluminosilicate dissolution from the MINTOX simulations therefore leads to inaccurate calculations of aqueous concentrations of these species. Also, the significance of reactions involving later precipitation and dissolution of secondary minerals (i.e., pH buffering) containing these components will be inaccurate. As part of this investigation, we tested the hypothesis of Johnson et al. (2000) that the precipitation and dissolution of secondary Al oxyhydroxide minerals (gibbsite) controls Al movement and buffers the pH near 4.

Table 1
Initial mineral phase concentrations in the tailings and aquifer. As the water moves and evolves, each mineral may dissolve or precipitate to maintain the water at equilibrium
Solid phase concentrations are in terms of moles of solid per 1000 g water, unless indicated otherwise.

Mineral	Oxidation zone of tailings	Aquifer, dam deeper tailings
Dolomite	0.08	0.08
Siderite	0.25	0.25
Gibbsite	0.2	0.25
Ferrihydrite	0	0
Gypsum	0	0
K-jarosite	0	0.01
Pyrrhotite (MINTRAN)	0	3 wt.%
Pyrite (MINTOX)	5.8 wt.%	0

Aluminum oxyhydroxides (primary or secondary) were not identified at Nickel Rim. In the place of aluminosilicates, a small quantity of gibbsite (0.4 wt.%) was included in the initial composition of tailings and aquifer to provide a limited and controlled source of Al for later gibbsite reprecipitation and dissolution (Table 1). Johnson et al. (2000) also suggest that jarosite precipitation and dissolution limits dissolved K and Fe^{3+} concentrations and buffers the pH at values between 2 and 3. A small amount of jarosite (0.1 wt.%) was included in the initial composition of the background solids, to provide a limited and controlled source of K (Table 1). If the conceptual model is correctly implemented, distinct pH buffering due to the precipitation and dissolution of secondary gibbsite and jarosite should be evident in the simulation results.

With the exception of siderite, the thermodynamic database of MINTEQA2 was adjusted to be consistent with that of WATEQ4F (Ball and Nordstrom, 1991). Ptacek (1992) found that the solubility product for siderite varies with the temperature of precipitation, and with the extent of solid-solution substitution. For the purpose of these simulations, the solubility product of siderite was increased to be in agreement with field-determined ion activity products of dissolved Fe^{2+} and CO_3^{2-} ($K_{sp} = 10^{-9.8}$).

4.3. Composition of background and infiltration water

The composition of the aquifer and tailings pore-water, prior to sulfide oxidation, is unknown. At the start of sulfide oxidation, 7 years after tailings discharge was initiated, mill discharge-water is assumed to have been uniformly distributed throughout the tailings and the aquifer. The aqueous chemistry of water samples collected from deep areas of the tailings near the flow divide (1993–1995) was assumed to be typical of the mill discharge-water. The composition of the background water used in MINTOX is shown in Table 2.

To simplify interpretation of plume development, water infiltrating the surface of the tailings and the aquifer is assumed to have a chemical composition similar to that of natural background water. For these simulations, the composition of natural groundwater found in a glaciofluvial aquifer at the Nordic Main tailings site, near Elliot Lake was used (Table 2; Morin, 1983).

4.4. Flow model

Nonreactive solute transport (PLUME2D) in MINTOX is based on steady state groundwater velocity vectors calculated for the flow system with the FNPCG flow model (Frind and Molson, 1992). Boundary conditions and other parameters used in the flow model are based on field and lab measurements of Johnson (1993) and Bain (1996), and are illustrated on Fig. 6a. The flow net generated for the Nickel Rim tailings impoundment and aquifer (Fig. 6b) was used to represent groundwater flow conditions at the site.

Two-dimensional flow codes do not adequately account for transverse horizontal groundwater flow, thus the simulated flow paths and groundwater velocities probably

Table 2
Aqueous geochemical composition (mol/l) of infiltration water and initial condition pore water in the tailings and aquifer. These are equilibrated compositions of field-sampled water collected in areas that contain mill-discharge water from the 1950s. The water was equilibrated with MINTEQA2 assuming dolomite, gibbsite, gypsum and siderite were present

Component	Background water	Infiltration water
Ca	1.32e−02	7.00e−03
Mg	2.51e−02	2.00e−03
Na	1.09e−02	1.30e−03
K	6.10e−03	2.60e−04
Cl	4.25e−04	3.00e−03
CO_3	1.07e−02	3.90e−03
SO_4	3.54e−02	6.00e−03
Fe^{2+}	2.57e−05	5.30e−05
Fe^{3+}	1.26e−08	7.90e−08
Al	5.82e−09	1.00e−08
H^+	1.35e−02	5.68e−03
HS^-	1.00e−06	1.00e−06
S^{2-}	1.00e−06	1.00e−06
pH	6.65	6.65
pe	3.56	3.56

represent conditions at the site only in a general sense. After 35 years in the modelled flow system, all water infiltrating between the dam and NR 6 is displaced out of the impoundment, and water that infiltrated near the flow divide is present near the base of the impoundment. At >60 m downgradient of the dam, the width of the aquifer increases by two to three times (Fig. 1). Groundwater flow paths are representative in this area, but velocities are probably overestimated.

4.5. Transport model

The domain for the reactive transport modelling is 360 m by 6 to 9 m. The finite element grid consists of 7740 rectangular elements, numbering 30 vertical and 258 horizontal. For simplicity, velocities in the unsaturated zone are assumed to be vertical.

The bedrock and flow divide are zero-concentration gradient boundaries. The water table in the tailings is a type III (Cauchy) transport boundary. The composition of the water crossing the tailings water table in the tailings is determined after every time step by MINTOX. The water table in the aquifer is a type III transport boundary.

Parameters in the transport portion of the model include longitudinal (α_x) and transverse (α_z) dispersivities of 4.5 and 0.07 m, respectively, an effective molecular diffusion coefficient (D^*) of 5.05×10^{-3} m^2/a and uniform tailings and aquifer porosity of 0.4 (Table 3).

4.6. Boundary conditions for the sulfide oxidation model (PYROX)

Sulfide (pyrite) oxidation is restricted to the unsaturated zone of the tailings, within 0.7 m of the tailings surface, where oxygen is replenished by gas-phase diffusion.

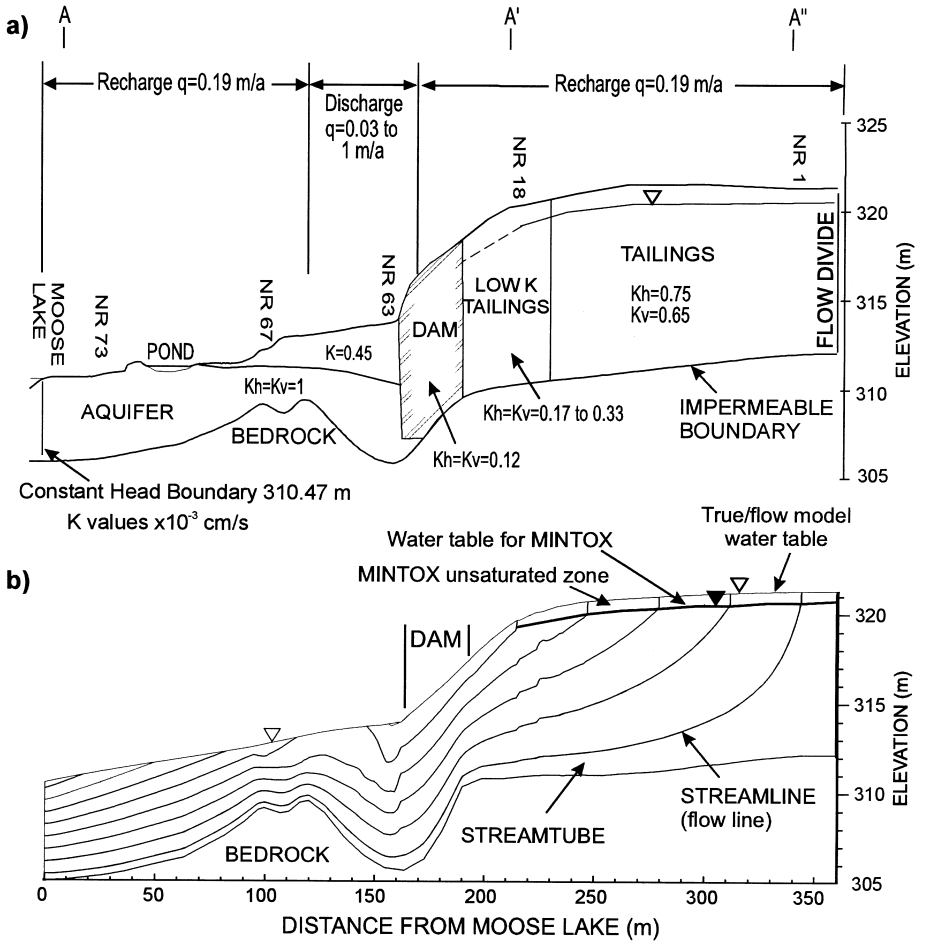

Fig. 6. (a) Boundary conditions and hydraulic conductivity zones for the flow system and (b) flow net generated with FNPCG for use in the transport portion of MINTOX. Stream tubes on the flow net represent flow paths.

Between 1991 and 1992, the average depth to the water table in the tailings is approximately 1 m (Johnson, 1993). Although the vadose zone was probably thinner immediately after decommissioning, in the oxidation model, the thickness is assumed to be constant at 1 m. The surface of the tailings is considered to be a constant concentration boundary for oxygen (Type I, Dirichlet), with the atmospheric concentration equal to 20.9% by volume. In PYROX, the water table and lateral boundaries of the vadose zone of the tailings represent zero concentration gradient boundaries (Type II, Neumann) for the diffusion of oxygen.

The rate of oxygen diffusion, and subsequently, the rate of sulfide oxidation in the tailings pore space is dependent on the bulk diffusion coefficient (D_1) of oxygen in the

Table 3
Parameter values for the sulfide oxidation and solute transport routines of MINTOX. Parameters selected result in a good fit of observed and modelled S and O_2 content of the vadose zone of the tailings at NR 18 (Bain, 1996)

Parameters used in PYROX/MINTOX	Value
Pore space O_2 diff. coeff. D_1 (m^2/s)	Determined from moisture content
Oxide coating O_2 diff. coeff. D_2 (m^2/s)	3.90e−14
Sulfide particle radius (m)	7.60e−05
Porosity	0.415
Tailings bulk density (g/l)	1550
Wt.% S (wt.% pyrite)	3.1 (5.8)
Thickness oxidation zone (m)	1
Oxidation time step (years)	0.001
Longitudinal dispersivity (m)	4.5
Transverse dispersivity (m)	0.07
Molecular diffusivity (m^2/s)	0.005
MINTRAN time step (years)	0.08

pore space of the tailings. This value is dependent on the moisture content of the tailings. PYROX uses the moisture content of a vertical column of tailings, measured at a representative location in the unsaturated zone (NR 18; Johnson, 1993), to determine these D_1 values during the simulations.

The rate of sulfide oxidation is dependent, in part, on the rate at which oxygen diffuses through the alteration rim surrounding the sulfide grains. The oxygen diffusion coefficient of these oxide coatings (D_2) cannot be determined independently (Wunderly et al., 1996). Sensitivity analyses suggest that an oxygen diffusion coefficient (D_2) of 3.9×10^{-14} m^2/s for the oxidized coatings on the sulfide grains results in depletion of sulfides in the oxidation zone representative of current field observations (Bain, 1996).

For the sulfide oxidation calculations, a porosity value of 0.41, representative of the average measured porosity in the unsaturated zone (Johnson, 1993), was used for the full thickness of the unsaturated zone. Oxygen diffusion into the tailings is assumed not to occur during the winter months due to the barrier presented by snow cover and frozen ground. It has been specified, therefore, that PYROX generates sulfide oxidation products for only half of a year. The oxidation of sulfides below the vadose zone by Fe(III) occurs continuously within the geochemical equilibrium (MINTEQA2) portion of MINTOX. Additional parameters for the simulation of sulfide oxidation are listed in Table 3. Although pyrite oxidation is simulated as a surrogate for pyrrhotite, with the sulfide oxidation parameters selected, the fit of observed and measured sulfur content and O_2-diffusion profiles in the vadose zone at NR 18 are good (Bain, 1996).

5. Results and discussion

5.1. MINTOX simulation results

The simulation represents 35 years of sulfide oxidation and plume development, from 1959 (decommissioning) until 1994, when field monitoring was in progress (Johnson,

1993; Bain, 1996). The results are presented in 2-D cross-sections (Figs. 7–9), with 1-D vertical profiles (Fig. 10) of the simulated data near NR 6 in the impoundment (≈ 300 m from Moose Lake). The modelled plume development after 35 years may be compared to the results of the field observations, presented for NR 6 and NR 18 on the 1-D vertical profiles. Fig. 11 shows how the modelled dissolved and solid phase concentrations and pH at a point in the oxidation zone near NR6 change over time.

5.1.1. Simulated transport of conservative species

In the simulations, Cl is transported conservatively. The constant source is 0.003 mol/l. The Cl plot serves as a basis of comparison of the movement of the various constituents undergoing reactive transport, and indicates the maximum extent of the plume originating in the impoundment (Fig. 7).

5.1.2. Simulated plume development

Figs. 8 and 9 illustrate the simulated movement of dissolved species and the development of mineral precipitation/dissolution zones after 10 and 35 years of reactive transport. A comparison of the figures indicates that high concentrations of Fe(II) and SO_4 are produced during the first 10 years of simulated oxidation. Afterwards, lower concentrations of Fe and SO_4 are produced, due to depletion of sulfide minerals in the vadose zone, and due to the increasing thickness of the alteration rim surrounding the sulfide particles. This decrease in oxidation rate results in slug-like movement of older

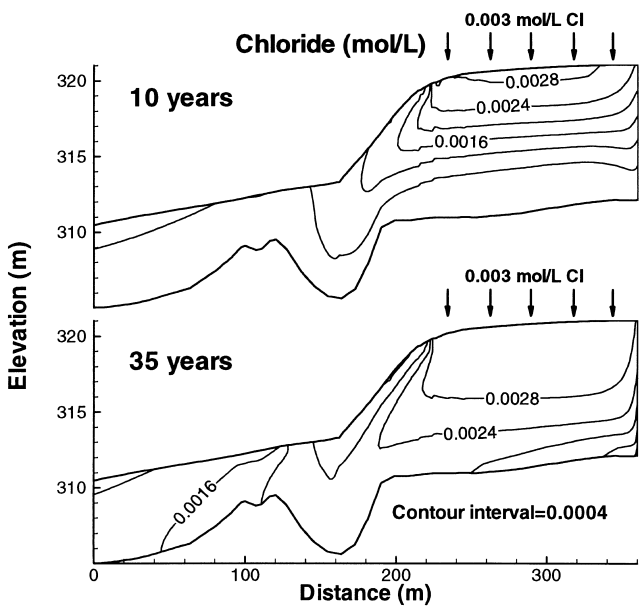

Fig. 7. Simulated evolution of a Cl plume at 10 and 35 years, under a constant source of 0.003 mol/l Cl.

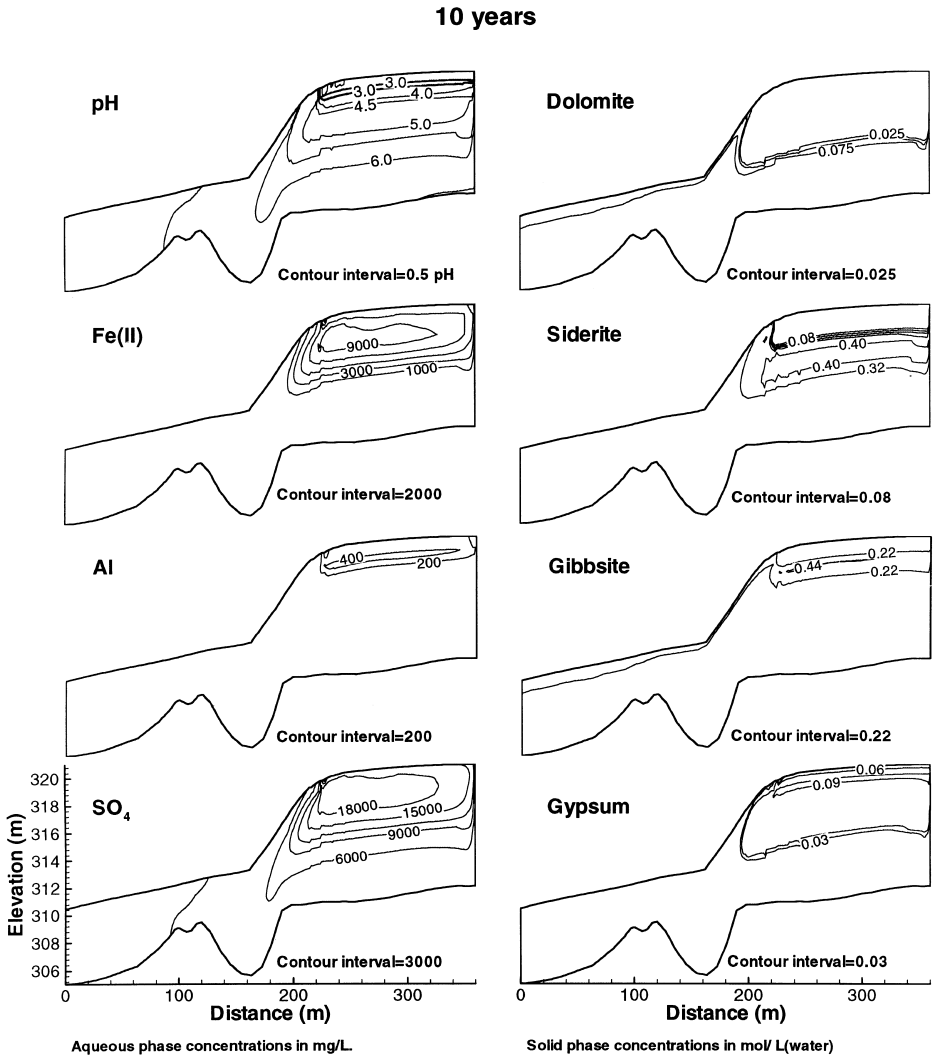

Fig. 8. 2-D plots of pH, aqueous and solid phase concentrations after 10 years of simulated reactive transport.

water with high concentrations of Fe(II) and SO_4 toward the base of the impoundment (Figs. 8 and 9). In the simulation, Fe and SO_4 form a plume in the tailings and aquifer with concentrations that are consistent with the conditions observed in the field (Fig. 3). Trends in the simulated pH conditions (Figs. 8 and 9) are similar to those measured in the tailings and aquifer, although lower values are attained. These lower pH values arise because MINTOX does not account for CO_2 degassing and upward diffusion of CO_2 through the vadose zone. At the mid-tailings location (NR 6) the vertical distribution and concentrations of the major ions Al, Ca, Fe, and SO_4 after 35 years agree well with field-measured values (Fig. 10).

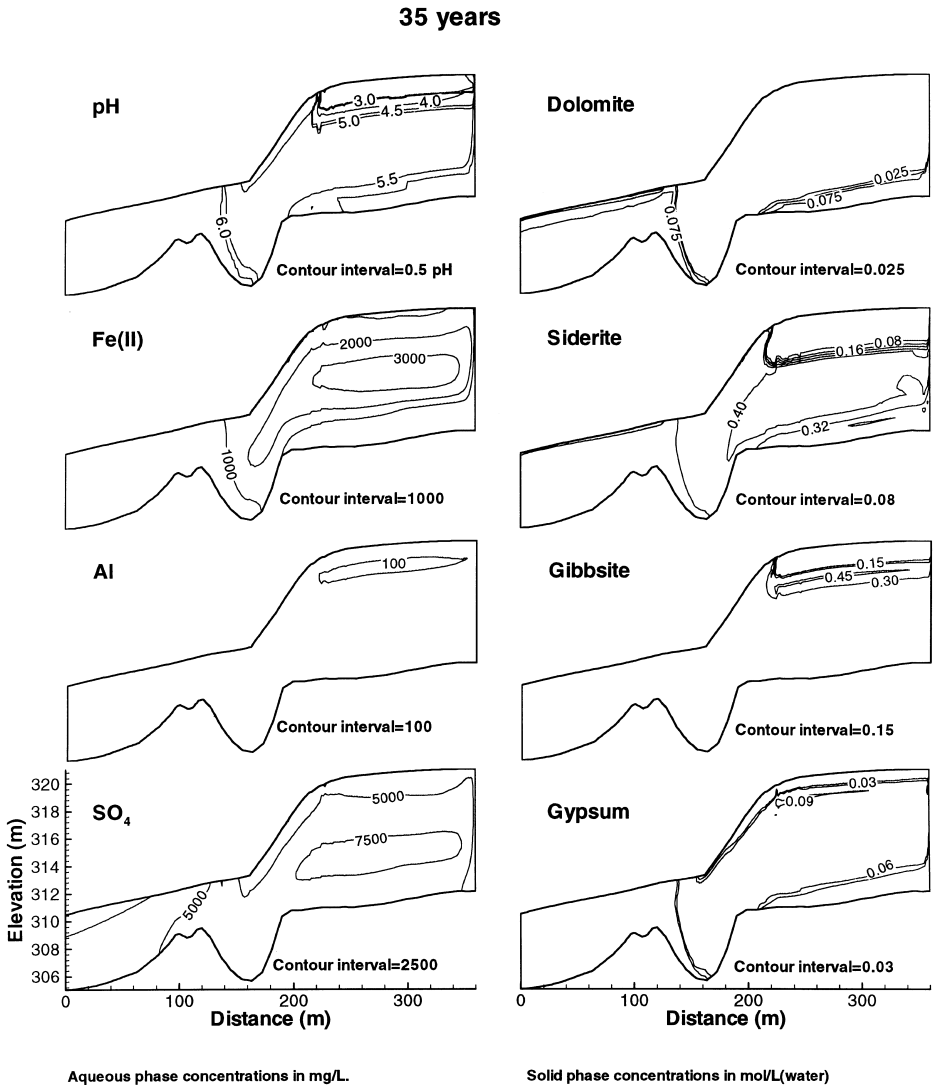

Fig. 9. 2-D plots of pH, aqueous and solid phase concentrations after 35 years of simulated reactive transport.

The simulation shows an isolated zone of high Fe and SO_4 concentrations 4 to 5 m below the oxidation zone after 35 years, similar to the field observations (Figs. 9 and 10). The position of the zone of highest concentrations is slightly shallower (1 to 2 m) than in the field (Figs. 3 and 10), indicating either that the modelled groundwater flow velocities in the tailings are slightly low, or that sulfide oxidation started at the site at an earlier time. Differences in the observed and simulated position of the plume may also arise because variations in the historic rate of sulfide oxidation are not accounted for in

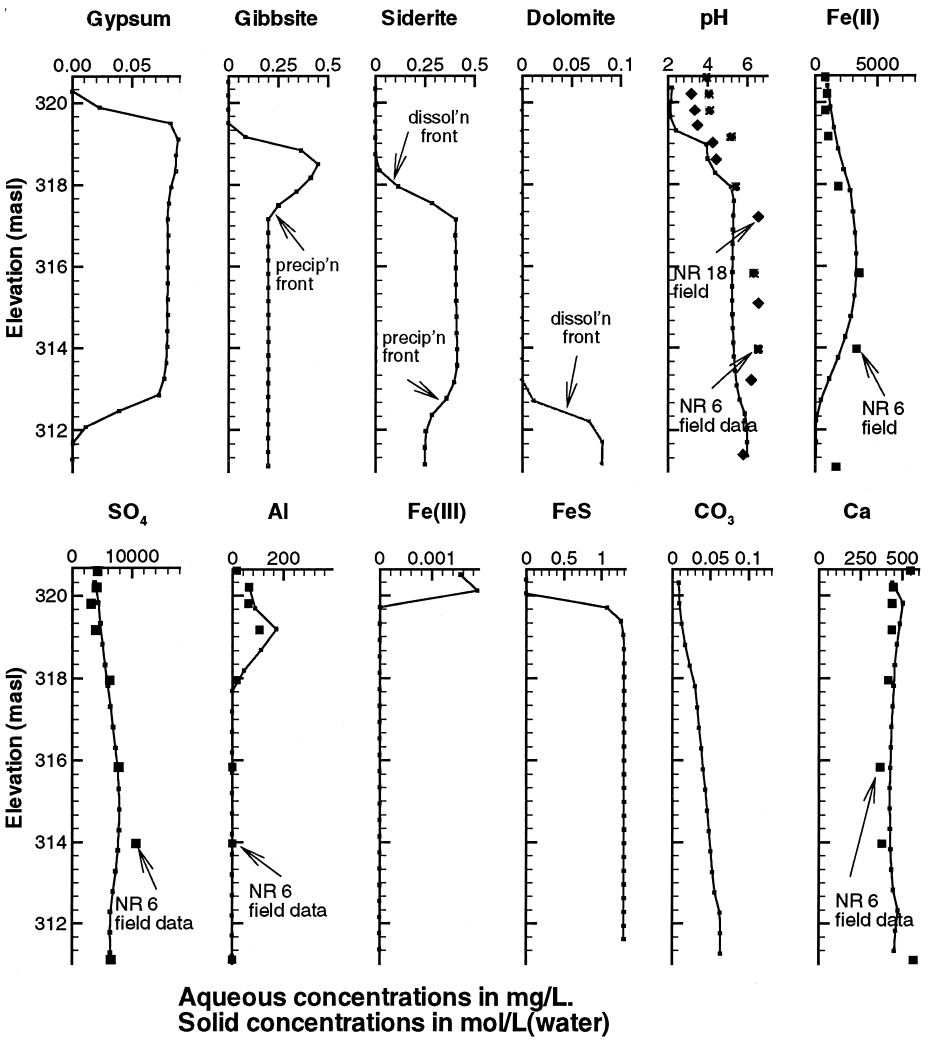

Fig. 10. Depth plots of simulated pH conditions, aqueous species and solid phase concentrations at 35 years. Selected field data collected at NR 6 is plotted for comparison.

MINTOX. In the model, oxidation products are generated for half a year at a time with no transient variations.

Simulated development of the plume in the aquifer is not as accurate as in the tailings. These differences probably reflect discrepancies between the natural and modelled flow systems, particularly downgradient of the tailings dam. It may be possible to fit the observed and modelled plumes exactly by adjusting the modelled flow system. The goal of the simulations, however, is to demonstrate that the conceptual model for the site is reasonable and that MINTOX is capable of simulating this conceptual model.

5.1.3. Simulated evolution of low-pH conditions and the mobility of dissolved metals

Several plateaus, where the pH is relatively constant, are evident in the 1-D vertical profiles (Fig. 10) and breakthrough plots (Fig. 11). In the simulation, the plateaus occur at pH values of approximately 6.0, 5.0, 3.9, 3.0 and 2.1. The pH 3 plateau is more distinct at 10 years than at 35 years. Between these plateaus, the pH decreases sharply, stepwise, with the dissolution of dolomite (pH ≈ 6), and the secondary minerals siderite (pH ≈ 5), gibbsite (pH ≈ 3.9) and ferrihydrite (pH ≈ 3; Figs. 8 and 9). The pH 2.1 plateau occurs after the dissolution of ferrihydrite, and probably represents the rate of H^+ production by sulfide oxidation. These pH-plateaus and sharp pH-changes are in agreement with trends in the field, although the pH values are slightly lower than the

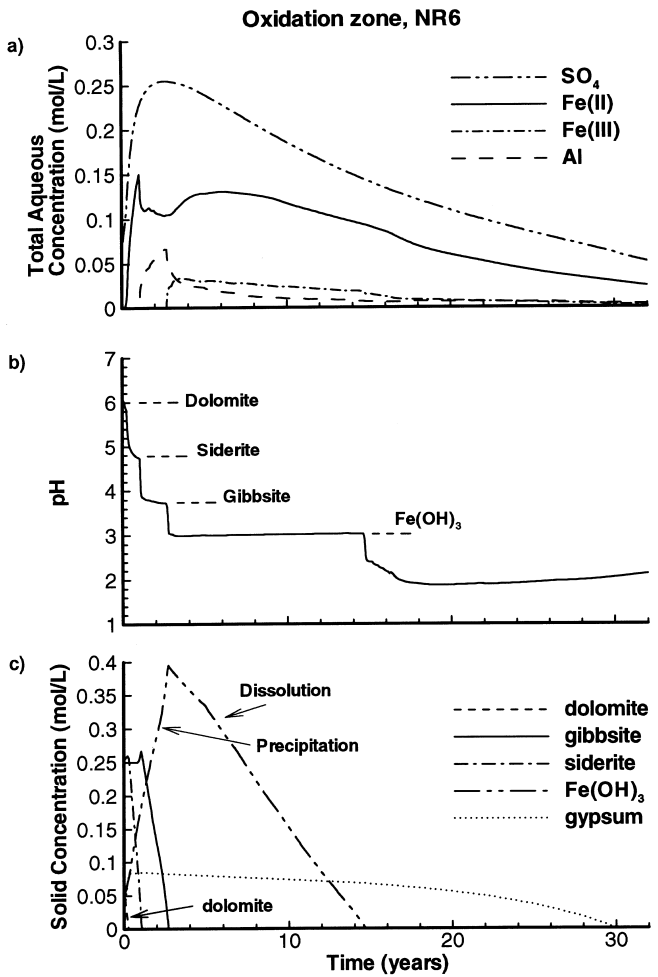

Fig. 11. Breakthrough curves for selected aqueous and solid phase species at point 1, 15 cm below the base of the oxidation zone, near NR 6.

values observed in the field. Lower pH-plateau values in the simulation probably result from differences between the composition of pH-buffering phases at the site and in the model, and the inability of the model to account for CO_2 degassing, discussed above.

Dolomite is the first mineral to dissolve upon the infiltration of low-pH water from the oxidation zone (Fig. 11). After 35 years, the zone of dolomite depletion (Fig. 9) includes the main part of the tailings and a small part of the aquifer near the dam, similar to conditions currently observed in the field. Downgradient of the dolomite dissolution front, dolomite dissolution buffers the pH to near-neutral (≈ 6). Where dolomite dissolves, infiltrating Fe(II), derived from sulfide oxidation, reacts with the CO_3 released by acid neutralization, resulting in the precipitation of siderite (Figs. 10 and 11). As the dolomite dissolution/siderite precipitation front moves downgradient, siderite accumulates.

Although the pH and buffering solids behaviour is in agreement with field conditions, the Fe(II) distribution is inaccurate beyond the dolomite dissolution front. Downgradient of the dolomite dissolution front the simulated Fe(II) concentration is < 10 mg/l (Figs. 8 and 9). At the field site, much higher Fe(II) concentrations (500–2000 mg/l) persist downgradient of the tailings dam, in areas where mixed composition dolomite dissolution buffers the pH to near-neutral (≈ 6; Fig. 3). Fe(II) movement in the simulation may be inhibited due to the dissolved carbonate concentration which, in this simulation, is slightly higher than at the field site. Also, MINTOX does not presently incorporate partitioning of CO_2 into the pore space of the vadose zone of the tailings or the subsequent upward diffusion of CO_2 (gas). As a result, greater concentrations of dolomite are dissolved in the simulation, generating high total dissolved CO_3 (0.02–0.06 mol/l) concentrations in the tailings water. These CO_3 concentrations are up to an order of magnitude higher than observed in the field (≈ 0.001–0.005 mol/l; Johnson, 1993). The high dissolved CO_3 concentrations cause extensive precipitation of siderite, and excessive attenuation of Fe(II) compared to field conditions. High concentrations of Fe(II) at the site may also exist if siderite and dolomite dissolution are kinetically limited. Alternatively, a siderite solid-solution phase that is more soluble than the pure siderite in the MINTOX database ($K_{sp} = 10^{-9.8}$) may control the Fe(II) concentration at the site.

After dolomite is depleted, the pH decreases sharply and stabilizes at between 4.8 and 5.1 (Fig. 11). Acidic water infiltrating from the oxidation zone is buffered to this pH by the dissolution of siderite. The water is near equilibrium with respect to siderite, as indicated by the constant siderite and CO_3 concentrations and stable pH values (Fig. 10). As observed by Johnson et al. (2000), this zone accounts for a major part of the impoundment. Dissolved Fe(II) concentrations reach maximum values at the siderite dissolution front. The siderite dissolution/precipitation front migrates downgradient as low-pH water infiltrates from the vadose zone (Fig. 10). Fe(II) concentrations decrease toward the base of the impoundment, reflecting the initially lower rates of sulfide oxidation.

Gibbsite, which was included in the initial background solids as a source of Al, dissolves after siderite is depleted (i.e., upgradient of the siderite depleted zone; Fig. 11). Al released at the gibbsite dissolution front is transported downgradient, until it reaches the siderite dissolution front (~ 317.6 m elev., Fig. 10), where higher pH conditions

cause the Al to reprecipitate as secondary gibbsite. Over time, this process results in secondary gibbsite concentrations that exceed the initial background concentration. As low pH water infiltrates from above, the accumulated secondary gibbsite dissolves, buffering the pH of infiltrating water to near 4 ($\sim$ 319 m elev., Fig. 10). The pH trends in the vicinity of the gibbsite dissolution front generally agree with field observations. The dissolved Al distribution after 35 years is similar to the distribution currently observed in the field (Fig. 10). At the field site, the first occurrence of carbonate minerals is accompanied by a sharp decrease in Al concentrations near the siderite pH-buffering zone and a change in the equilibrium state of pore-water with respect to gibbsite from supersaturated to undersaturated (Johnson et al., 2000).

Where the pH is < 5, Fe(II) concentrations are limited by the rate of sulfide oxidation, and the availability of oxygen, which oxidizes Fe(II) to Fe(III) (Eq. (4)). Within the first several years of the simulation, high oxygen concentrations near the surface of the tailings oxidize Fe(II) and generate high concentrations of Fe(III). At this time, the pH at these depths (< 0.7 m) is buffered by gibbsite, siderite or dolomite dissolution. The high Fe(III) concentrations result in ferrihydrite precipitation in the oxidation zone (Fig. 11). In the simulation, $Fe(OH)_3$ is precipitated only to a depth of about 0.7 m below surface. In agreement with field observations, this precipitation of ferrihydrite at pH > 3.8 limits the concentrations of dissolved Fe(III) in the oxidation zone.

When gibbsite is depleted, the ferrihydrite dissolution begins. Ferrihydrite dissolution buffers the pH near 3 and releases high concentrations of Fe(III) (up to 1600 mg/l; Fig. 11). In the simulation, ferrihydrite is depleted from the oxidation zone after about 15 years. Afterwards, the Fe(III) concentrations at shallow depths (< 0.6 m) in the tailings decrease gradually, as the rate of sulfide oxidation decreases, and less Fe(II) is produced. Upon the depletion of ferrihydrite, the pH within the oxidation zone decreases sharply to between 1.8 and 2.0 (Fig. 11).

Complete depletion of ferrihydrite in the tailings is not observed at the field site. At the field site, it is inferred that ferrihydrite first precipitated in the tailings, and subsequently transformed slowly into the more stable ferric oxyhydroxide mineral, goethite (Johnson, 1993). This transformation cannot be simulated with MINTOX because of phase rule constraints. Failure to incorporate the formation of goethite results in more rapid depletion of Fe(III)-bearing solid phases, and lower pH values in the oxidation zone (1.8–2.1) than are observed at the field site (pH $\approx$ 2.1–3.0; Fig. 3). Ferrihydrite was chosen in the simulations because field-data suggest that pH-buffering by ferrihydrite is important. The lower pH values simulated in the oxidation zone may also reflect the absence of aluminosilicate dissolution reactions in MINTOX. In the simulation, Fe(III) does not infiltrates below the depth where pyrrhotite is present (Fig. 10).

5.1.4. Simulated mobility of dissolved SO_4

In the simulation, SO_4 produced by sulfide oxidation is distributed through the tailings with few discontinuities (Figs. 8 and 9). The distribution of SO_4 in the tailings and aquifer approximates field observations (Fig. 3). SO_4 concentrations are partly limited in the simulation by the precipitation of gypsum. Elevated Ca concentrations at

the dolomite dissolution front (Fig. 10) promote gypsum precipitation. As the dolomite dissolution front progresses downward, a zone of secondary gypsum accumulates (Figs. 8–10). As the sulfides are depleted in the oxidation zone, the infiltration of water containing low concentrations of SO_4 dissolves gypsum from the surface downward. The groundwater throughout the majority of the impoundment is at equilibrium with respect to gypsum (Johnson et al., 2000). Low dissolved Ca concentrations and the high solubility of gypsum allow high SO_4 concentrations (6000 and 10,000 mg/l) to migrate out of the impoundment and into the aquifer.

5.2. Limitations in the simulations

Although major groundwater anions and cations were included, no attempt was made to correlate field data with the model results for ions other than H^+, Fe, Al, SO_4 and Ca. Several assumptions limit the ability of MINTOX to accurately simulate the pH conditions and plume features observed at the site. At the site, a wide variety of minerals exist and participate in reactions that control the aqueous chemistry of the water. For simplicity, the model has included only those phases assumed to dominate the pH conditions and concentrations of dissolved oxidation products. Due to differences in the composition of pH-buffering pure solids assumed in the simulation and the natural materials present at the field site, the solubilities of these pH-buffering solids also are different, affecting the pH.

Geochemical equilibrium may not be attained between flowing groundwater and adjacent solid phases, although in the model, this is assumed to occur. Although aluminosilicate mineral dissolution is believed to affect the pH and add dissolved components to the water (Johnson et al., 2000), these reactions are considered to be kinetically controlled, and are not simulated by MINTOX. The recently developed equilibrium/kinetic, reactive transport models HYDROGEOCHEM2 (Yeh and Salvage, 1997) and MIN3P (Mayer, 1999) should be able to account for the dissolution of minerals such as aluminosilicate minerals.

The oxidation of pyrite as a surrogate for pyrrhotite in the oxidation zone of the tailings will influence the concentrations of sulfide oxidation products generated. The current model does not account for historic variations in the thickness and moisture content of the vadose zone, and variations in the size and shape of sulfide grains, although these factors affect the diffusion properties of the tailings, and therefore the rate of pyrite oxidation. Groundwater flow in the unsaturated zone is assumed to be one-dimensional.

6. Conclusions

Sulfide oxidation started in the decommissioned Nickel Rim tailings approximately 35 years ago. A conceptual model of the mechanisms controlling the evolution of low-pH conditions, and of the mobility of dissolved metals and SO_4 in the impoundment and underlying aquifer was developed from data obtained in field investigations conducted at the site. This model accounts only for the dominant processes that control

the pH, metal and SO_4 behaviour. The multicomponent reactive transport model MINTOX simulated 35 years of pyrite oxidation, and the generation of Fe, SO_4 and H^+ in the tailings. Using data from the site and mechanisms described in a conceptual geochemical model for Nickel Rim, MINTOX simulated the development of low-pH conditions, and the movement of dissolved sulfide oxidation products in the tailings' impoundment and in an underlying aquifer. Processes simulated include sulfide mineral oxidation and the sequential dissolution of dolomite, siderite, gibbsite, ferric oxyhydroxide phases, and jarosite. Although the geochemical model as simulated by MINTOX is capable of describing plume development at the site, the solution is not unique.

MINTOX was able to simulate the mechanisms that are controlling pH conditions and metal and SO_4 mobility, although there are differences between the observed and simulated plume movement. These differences are attributed to discrepancies in the sulfide mineral oxidation rate, groundwater velocities and the composition of the background solids. The exclusion of aluminosilicate mineral dissolution from the model also adversely affects the results. The general agreement between the simulation results and the field observations suggests that MINTOX provides a useful tool for understanding the complex sequence of physical and chemical mechanisms that control plume development in mine drainage environments.

Acknowledgements

We thank Falconbridge for financial and laboratory support provided during the field investigation portions of this research. We also appreciate the assistance of John Molson (University of Waterloo), with model management, and Tom Al (University of New Brunswick), with constructive criticism. The authors thank the editor and two reviewers, B. Strömberg and an anonymous reviewer for their constructive comments.

References

Allison, J.D., Brown, D.S., Nova-Gradac, K.J., 1990. MINTEQA2/PRODEFA2, A geochemical assessment model for environmental systems: version 3.0 user's manual. Environmental Research Laboratory, Office of Research and Development, U.S. EPA, Athens, GA, 106 pp.

Bain, J.G., 1996. Hydrogeochemical investigation and reactive transport modelling of an aquifer affected by mine drainage. MSc thesis, University of Waterloo, Waterloo, Ontario.

Ball, J.W., Nordstrom, D.K., 1991. User's manual for WATEQ4F, with revised thermodynamic data base and test cases for calculating speciation of major, trace and redox elements in natural waters. U.S. Geological Survey, Open-File Report 91-183, 189 pp.

Blowes, D.W., Jambor, J.L., 1990. The pore-water geochemistry and the mineralogy of the vadose zone of sulfide tailings, Waite Amulet, Quebec, Canada. Appl. Geochem. 5, 327–346.

Blowes, D.W., Ptacek, C.J., 1994. Acid-neutralization mechanisms in inactive mine tailings. In: Jambor, J.L., Blowes, D.W. (Eds.), Short Course Handbook on Environmental Geochemistry of Sulfide Mine-Wastes. Mineralogical Association of Canada, pp. 271–292.

Blowes, D.W., Reardon, E.J., Jambor, J.L., Cherry, J.A., 1991. The formation and potential importance of cemented layers in inactive sulfide mine tailings. Geochem. Cosmochim. Acta 55, 965–978.

Blowes, D.W., Jambor, J.L., Appleyard, E.C., Reardon, E.J., Cherry, J.A., 1992. Temporal observations of the geochemistry and mineralogy of a sulfide-rich mine-tailings impoundment, Heath Steele Mines, New Brunswick. Explor. Min. Geol. 1 (3), 251–264.

Broshears, R.E., Runkel, R.L., Kimball, B.A., McKnight, D.M., Bencala, K.E., 1996. Reactive solute transport in an acidic stream: experimental pH increase and simulation of controls on pH, aluminum and iron. Environ. Sci. Technol. 30 (10), 3016–3024.

Cherry, J.A., Shepherd, T.A., Morin, K.A., 1982. Chemical composition and geochemical behavior of contaminated groundwater at uranium tailings impoundments. In: SME-AIME Annual Meeting, Dallas, TX — February 14–18, 1982. Preprint Number 82-114.

Davis, G.B., Ritchie, A.I.M., 1986. A model of oxidation in pyritic mine wastes: 1. Equations and approximate solution. Applied Mathematical Modelling 10, 314–322.

Dubrovsky, N.M., Morin, K.A., Cherry, J.A., Smyth, D.J.A., 1984. Uranium tailings acidification and subsurface contaminant migration in a sand aquifer. Can. J. Water Poll. Res. 19 (2), 55–89.

Filipek, L.H., Nordstrom, D.K., Ficklin, W.H., 1987. Interaction of acid mine drainage with water and sediments of West Squaw Creek in the West Shasta Mining District, California. Environ. Sci. Technol. 21 (4), 388–396.

Frind, E.O., Molson, J.W., 1992. FNPCG — steady state groundwater flow net model; version April 1992. Department of Earth Sciences, University of Waterloo, Waterloo, Ontario.

Frind, E.O., Duynisveld, W.H.M., Strebel, O., Boettcher, J., 1990. Modeling of multicomponent transport with microbial transformation in groundwater: the Furhberg case. Water Resour. Res. 26 (8), 1707–1719.

Jambor, J.L., Owens, D.R., 1993. Mineralogy of the tailings impoundment at the former Cu–Ni deposit of Nickel Rim Mines, eastern edge of the Sudbury Structure, Ontario. Mineral Sciences Laboratories Division Report MSL 93-4 (CF). CANMET, Energy, Mines and Resources, Canada.

Jaynes, D.B., Poinke, H.B., Rogowski, A.S., 1984. Acid mine drainage from reclaimed coal strip mines: 1. Model description. Water Resour. Res. 20 (2), 233–242.

Johnson, R.H., 1993. The physical and chemical hydrogeology of the Nickel Rim Mine tailings, Sudbury, Ontario. MSc thesis, University of Waterloo, Waterloo, Ontario.

Johnson, R.H., Blowes, D.W., Robertson, W.D., Jambor, J.L., 2000. The hydrogeochemistry of the Nickel Rim Mine tailings impoundment. J. Contam. Hydrol. 41, 49–80, Sudbury, Ontario.

Mayer, K.U., 1999. A numerical model for multicomponent reactive transport in variably saturated porous media. PhD thesis, Department of Earth Sciences, University of Waterloo, Waterloo, Ontario.

Morin, K.A., 1983. Prediction of subsurface contaminant transport in acidic seepage from uranium tailings impoundments. PhD thesis, Vols. I and II, Department of Earth Sciences, University of Waterloo, Waterloo, Ontario.

Morin, K.A., Cherry, J.A., Davé, N.K., Lim, T.P., Vivyurka, A.J., 1988. Migration of acidic groundwater seepage from uranium-tailings impoundments: 1. Field study and conceptual hydrogeochemical model. J. Contam. Hydrol. 2, 217–303.

Nicholson, R.V., 1994. Iron-sulfide oxidation mechanisms: laboratory studies. In: Jambor, J.L., Blowes, D.W. (Eds.), Short Course Handbook on Environmental Geochemistry of Sulfide Mine-Wastes. Mineralogical Association of Canada, pp. 163–183.

Ptacek, C.J., 1992. Experimental determination of siderite solubility in high ionic-strength aqueous solutions. PhD thesis, Department of Earth Sciences, University of Waterloo, Waterloo, Ontario.

Ptacek, C.J., Blowes, D.W., 1994. Influence of siderite on the pore-water chemistry of inactive mine-tailings impoundments. In: Alpers, C.N., Blowes, D.W. (Eds.), Environmental Geochemistry of Sulfide oxidation. ACS Symposium Series 550, pp. 172–189.

Rubin, J., 1983. Transport of reacting solutes in porous media: relation between Mathematical nature of problem formulation and chemical nature of reactions. Water Resour. Res. 19 (5), 1231–1252.

Stumm, W., Morgan, J.J., 1981. Aquatic Chemistry — an Introduction Emphasizing Chemical Equilibria in Natural Waters, 2nd edn. Wiley, New York, 780 pp.

Thomson, Jas.E., 1961. MacLennan and Scadding Townships. Geological Report No. 2, Ontario Dept. of Mines, pp. 25–27.

Walter, A.L., Frind, E.O., Blowes, D.W., Ptacek, C.J., Molson, J.W., 1994a. Modeling of multicomponent reactive transport in groundwater: 1. Model development and evaluation. Water Resour. Res. 30 (11), 3137–3148.

Walter, A.L., Frind, E.O., Blowes, D.W., Ptacek, C.J., Molson, J.W., 1994b. Modeling of multicomponent reactive transport in groundwater: 2. Metal mobility in aquifers impacted by acidic mine tailings discharge. Water Resour. Res. 30 (11), 3149–3158.

Wunderly, M.D., Blowes, D.W., Frind, E.O., Ptacek, C.J., 1996. Sulfide mineral oxidation and subsequent reactive transport of oxidation products in mine tailings impoundments: a numerical model. Water Resour. Res. 32 (10), 3173–3187.

Yeh, G.T., Salvage, K.M., 1997. HYDROGEOCHEM 2.0: a coupled model of hydrologic transport and mixed kinetic/equilibrium reactions in saturated/unsaturated media. Model user's guide issued September 1997.